

## 4. Creation and characterization of surface oxygen functionality

As mentioned previously in chapter 3, surface functionalization plays a significant role in the activity of carbon materials in the ODH reactions. Thus, the production of surface functional groups is an essential step in activating the HOPG samples.

The following different approaches were used in the aim to introduce surface functionality on HOPG surface.

- 1- The first approach based on the oxidation of HOPG surface by heating it in oxygen partial pressure under ultrahigh vacuum conditions ( $P$  up to  $\sim 1 \times 10^{-7}$  mbar).
- 2- The second approach based on creating surface defects by argon sputtering, followed by exposure to molecular oxygen. In this approach the aim was to create some defects on the surface of HOPG by the action of sputtering and expecting an interaction between these defects and molecular oxygen to which the sample was exposed directly after sputtering.
- 3- Finally, oxygen was used to sputter the sample either alone or mixed with argon in 1:1 mixture. In this treatment, the aim was that the high energy of the accelerated oxygen ions creates defects and reacts with these positions in the same step.

The surface was tested after every one of these treatments by Auger electron spectroscopy (AES) and by thermal programmed desorption (TPD).

Figure 4.1 is the AES spectrum of a clean (freshly cleaved and annealed) HOPG sample, the carbon signal appears at  $\sim 270$  eV. A very small signal appears of  $\sim 500$  eV. This signal which is just above the noise level of the spectrum can be caused by some oxygen-containing structures (ether-like structures) surviving the temperature of annealing. These very stable structures don't play any noticeable role in the catalytic properties of carbon materials in ODH reactions.

Additionally, no signal of Pt can be seen in the spectrum, this excludes the contribution of the platinum sample holder in this or any of the shown spectra.

#### 4.1 Thermal treatment in oxygen partial pressure

In the first approach based on heating the graphite in oxygen at UHV conditions, the clean annealed sample was heated up to 820 °C in  $8 \times 10^{-8}$  mbar oxygen for about 2 hours.  $^{18}\text{O}_2$  was used in order to distinguish the carbon oxides desorbing from the sample, from the carbon oxides desorbing from the sample holder and UHV parts which will contain the oxygen  $^{16}\text{O}$  isotope. The sample was left to cool to room temperature before it was subjected to analysis.

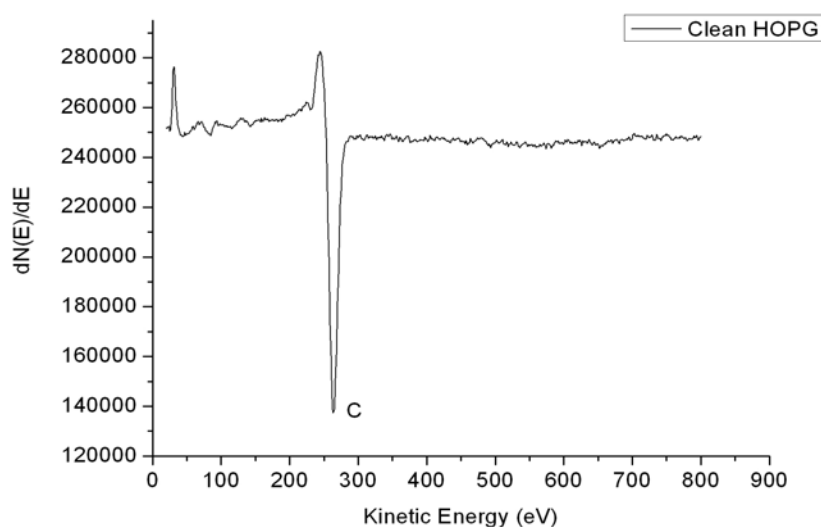


Figure 4.1. Auger spectrum of a clean HOPG sample

Figure 4.2 shows the AES spectrum of the HOPG sample after heat treatment in oxygen. The same tiny signal of oxygen which was discussed shortly above can be seen, but no signal of any created oxygen functionality can be detected in the spectrum, suggesting an oxygen-free surface. Figure 4.3 shows the TPD spectra of this sample. Broad peaks of CO (28 amu) and CO<sub>2</sub> (44 amu) appear at 250 °C and 150 °C, respectively. These signals should originate from the sample holder and other UHV parts and not from the sample itself because oxygen ( $^{18}\text{O}_2$ ) was used in this experiment. This and the previous results show that the used approach was unable to create oxygen functionalization on the surface. This is in agreement with the known properties of HOPG which is reported to be thermally stable.

## 4.2 Sputtering with argon and exposure to molecular oxygen

In the second approach, the clean sample was sputtered for 5 minutes with argon ( $2 \mu\text{A}$ ,  $1\text{keV}$ ). This step aims to create defects on the surface which are known to be unstable centres and can interact easily with molecules or atoms in the nearby. After switching the sputtering ion gun off and evacuating the system from argon, oxygen was admitted to the system ( $\sim 1$  min between stopping sputtering and reaching the required oxygen pressure) and the sample was exposed to  $1 \times 10^{-6}$  mbar oxygen for 15 minutes at RT. The direct exposure of the sputtered sample to oxygen excludes the possibility of saturation of the created defects by hydrogen from the UHV residual gas.

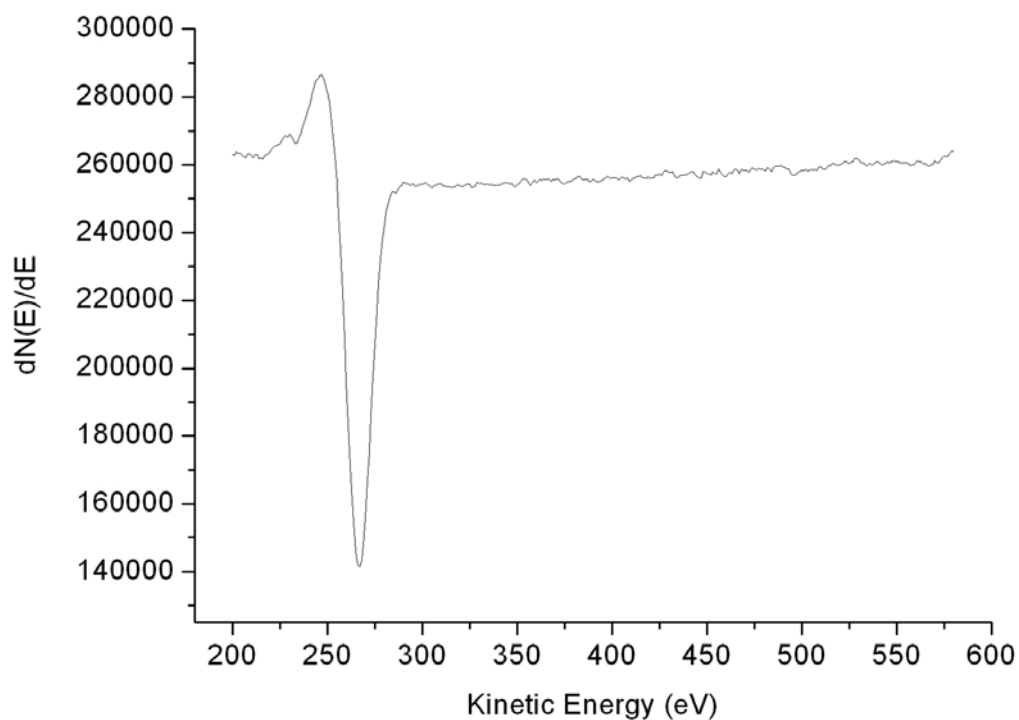


Figure 4.2. AES spectrum of HOPG substrate after heat treatment in oxygen at UHV condition

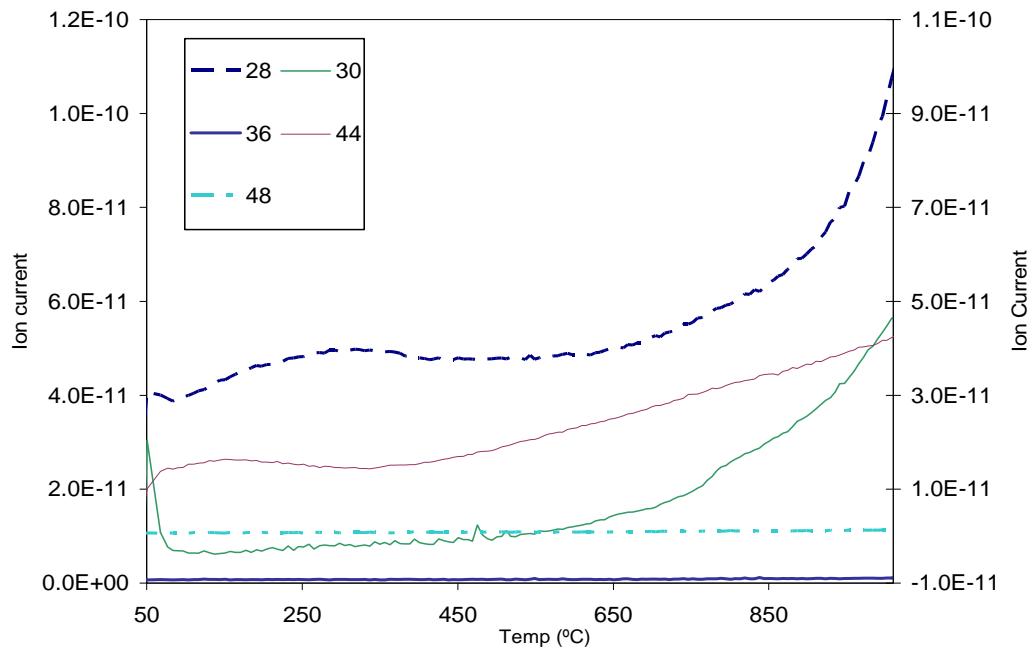


Figure 4.3. TPD Spectra of HOPG sample after heat treatment in oxygen atmosphere  
Molecular weights: 28 (CO), 30 (C<sup>18</sup>O), 36 (<sup>18</sup>O<sub>2</sub>), 44 (CO<sub>2</sub>), 48 (C<sup>18</sup>O<sub>2</sub>)

Figure 4.4 shows the AES spectrum of the sputtered sample after exposure to oxygen. Signals coming from carbon and argon are seen at 271 eV and 217 eV respectively. Again, no signal of oxygen is observed in the spectrum.

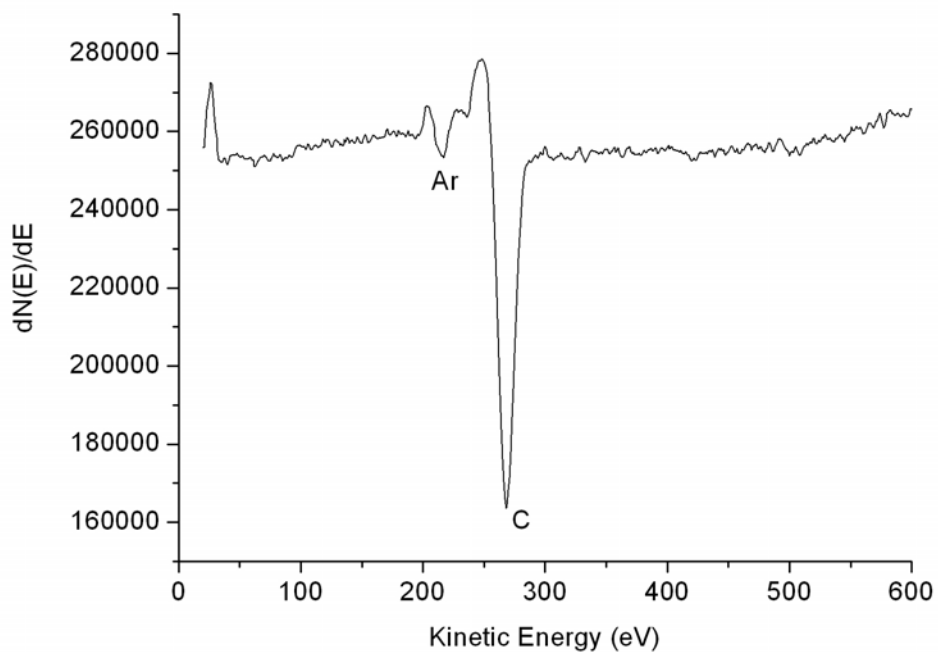


Figure 4.4. AES spectrum of argon-sputtered HOPG after exposure to oxygen

TPD spectra shown in figure 4.5 gave also the same indication, and no desorption peaks of either CO or CO<sub>2</sub> were observed. The very small features appearing in the CO desorption spectrum at 300 °C and 400 °C originate from sample holder since they are similar to what was observed in figure 4.3 in the signal of 28 amu.

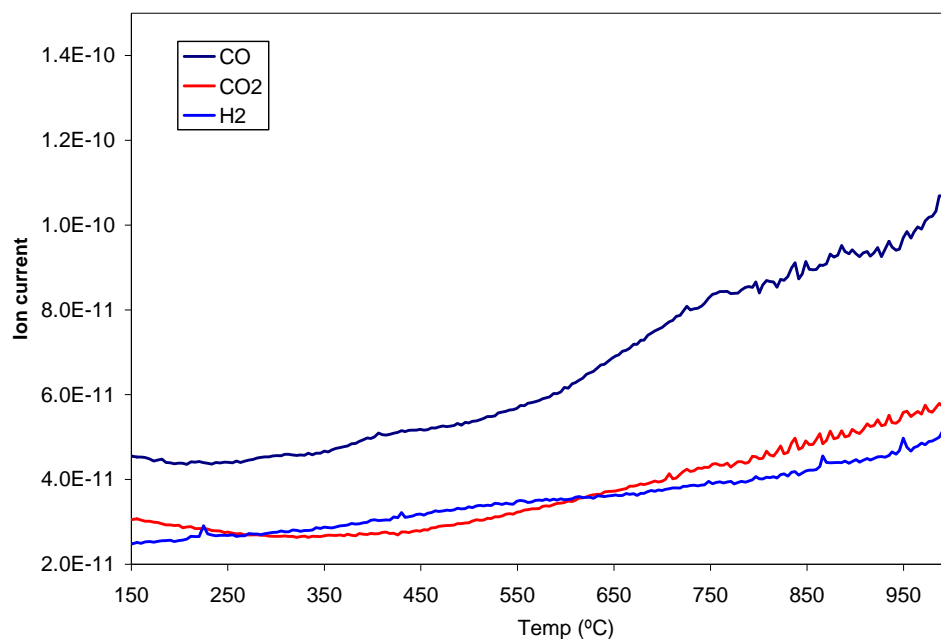


Figure 4.5. TPD Spectra of argon-sputtered HOPG after exposure to oxygen

### 4.3 Sputtering with oxygen

After the first and second approaches did not give any success in the production of surface oxygen functionalization, the third approach based on the sputtering of the HOPG surface with pure oxygen or oxygen/Argon mixture was applied. Figure 4.6 shows the AES spectrum of an HOPG sample which was sputtered with 1:1 oxygen (<sup>18</sup>O<sub>2</sub>)/argon mixture for 4 minutes (2 μA, 1 keV). In addition to the carbon signal at 270 eV, this AES spectrum shows now a clear signal of oxygen at (504 eV).

XPS technique was additionally used to investigate the oxygen-sputtered HOPG samples. In figure 4.7 an O1s XPS spectrum is shown. It can be easily seen that the spectrum is composed of at least two peaks, the first peak at 532.9 eV and the second at 530.8 eV. This provides an evidence of the presence of two or more

different oxygen containing species. The nature of these species, however, can not be deduced.

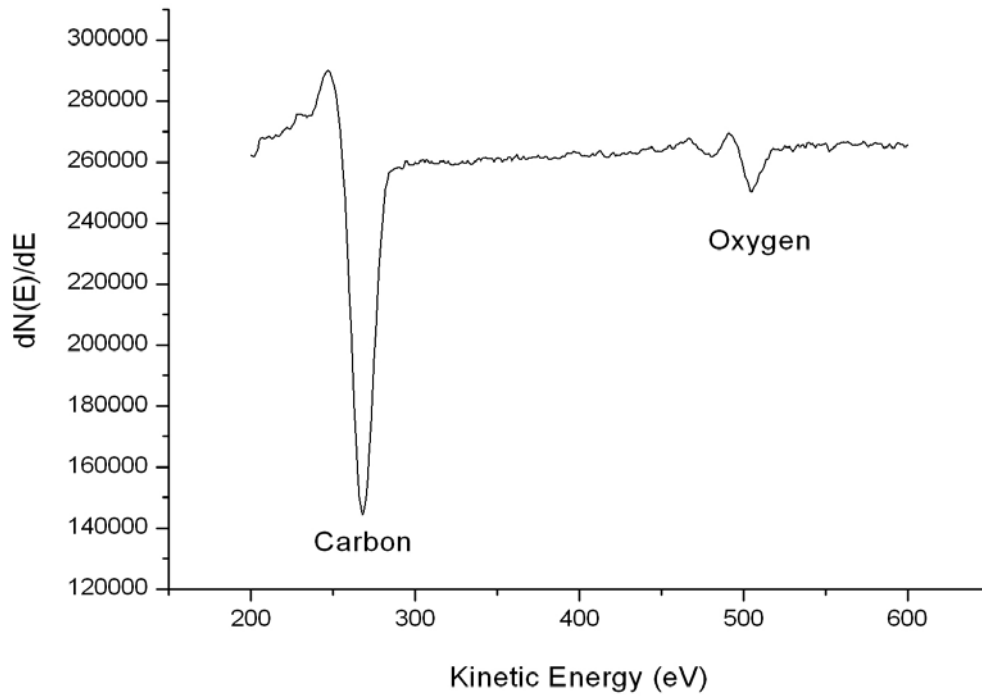


Figure 4.6. Auger after Sputtering 4 min, 1:1 Ox/Ar, 2 $\mu$ A, 1 keV

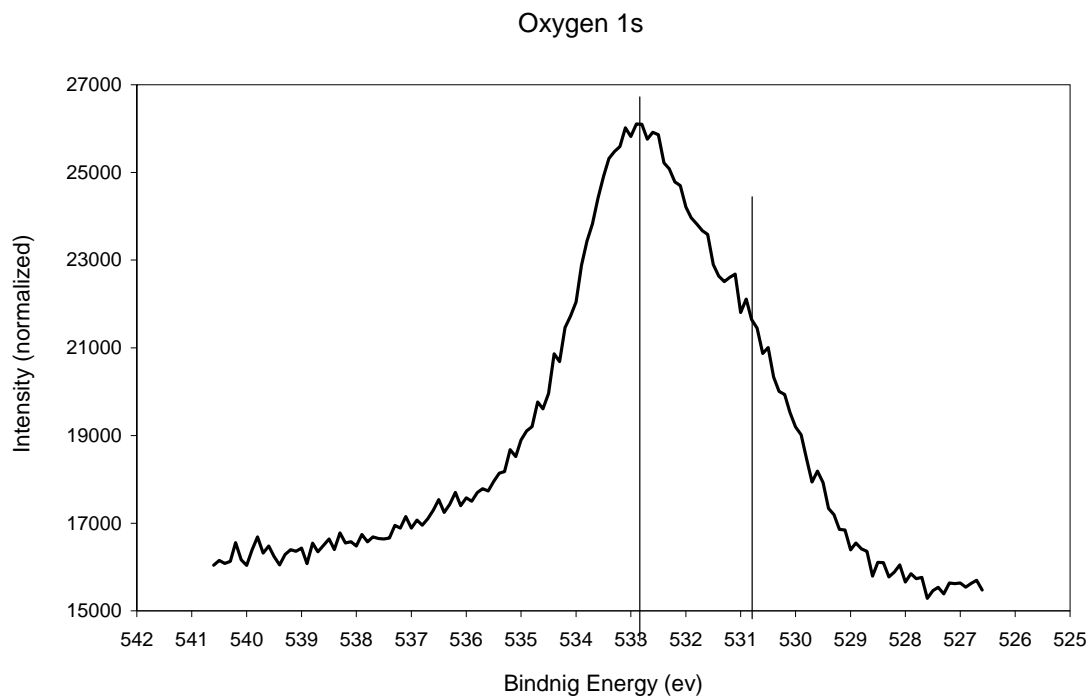
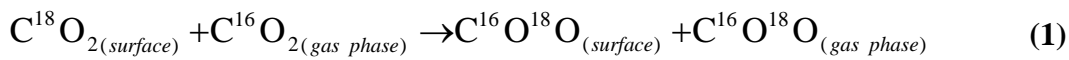


Figure 4.7 O1s XPS spectrum of oxygen-sputtered HOPG sample (5 min, 1 $\mu$ A, 1 keV)

In agreement with AES, TPD experiment revealed carbon monoxide and carbon dioxide peaks as the main desorption peaks (Fig 4.8).

As mentioned before, the CO (28 amu) and CO<sub>2</sub> (44 amu) signals do not originate from the sample since <sup>18</sup>O<sub>2</sub> was used in sputtering the sample. C<sup>18</sup>O (30 amu) peak appears at ~ 580 °C. C<sup>18</sup>O<sub>2</sub> (48 amu) peak appears at 480 °C. The signal of (46 amu) corresponds to CO<sup>18</sup>O. This can be a result of isotope exchange reactions<sup>1</sup>. The exchange can be between a surface oxygen complex resulting from sputtering (containing <sup>18</sup>O) and another one present originally in the structure of HOPG (containing <sup>16</sup>O). Another possible exchange reaction can occur between a surface oxygen complex and gas phase CO<sub>2</sub> present in the chamber rest gas as follows



The reaction above can –additionally– explain why the background signal of 46 amu is higher than that of 48 amu.

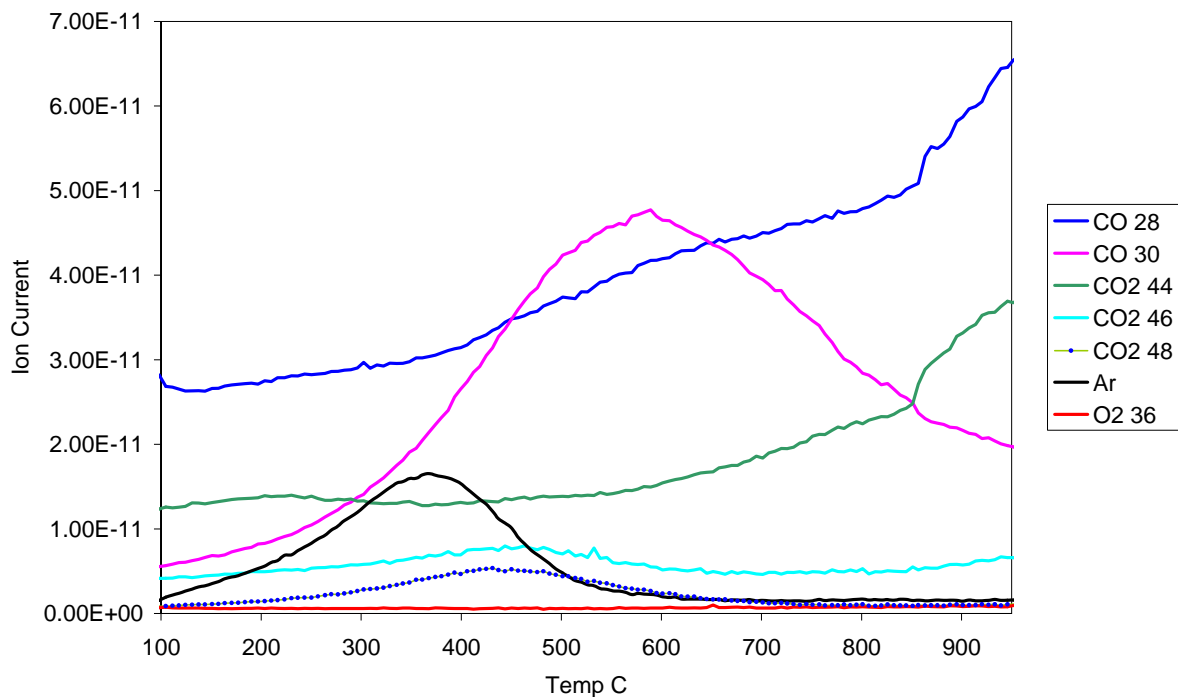


Figure 4.8 TDS Spectra of HOPG sample sputtered with 1:1 mixture of O<sub>2</sub>/argon.

Molecular oxygen desorption was also observed but with very low intensity compared to other species. This signal which is shown in figure 4.9 indicates the presence of physically adsorbed molecular oxygen which is the precursor for the oxygenated functional groups.

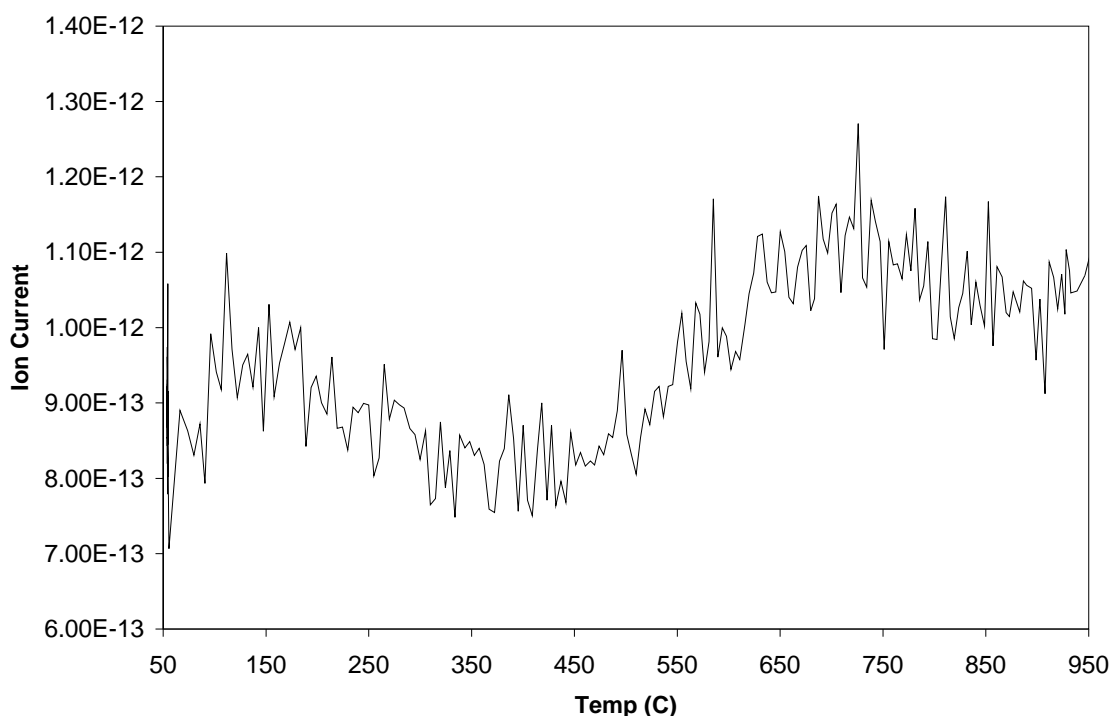


Figure 4.9 Oxygen TDS signal of HOPG sample sputtered with 1:1 mixture of O<sub>2</sub>/argon

Making any direct prediction of the types of the oxygenated groups present on the surface from the available desorption peak positions is not possible. Although some information about the characteristic desorption peaks' temperatures of some groups is available in the literature, this data vary widely from one group to another<sup>2</sup> and as explained in the third chapter, it depends on several experimental factors.

The influence of the sputtering time on the Auger signal of oxygen was studied. Figure (4.10) shows the Auger spectra recorded after sputtering the HOPG sample with oxygen/argon mixture for different durations using same ion current and ion energy. Taking the error range of these experiments into account, no influence can be seen of the sputtering time on the signal of oxygen in Auger spectroscopy.



This can also be clearly seen upon calculating the ratio of peak height (zero to bottom) of oxygen to that of carbon which is given in Figure 4.11. The calculated ratio obtained from a series of (sputter/anneal) experiments in which the sample was sputtered for 3, 6, 10 and finally 3 minutes. Ranges from 0.105 to 0.131 were observed separately but without any obvious correlation to the sputtering duration.

Considering the surface sensitivity of Auger spectroscopy, which is limited to few monolayers, the absence of any correlation between the sputtering duration and the detected amount of oxygen can be explained assuming that the top monolayers are saturated with oxygen at the beginning of sputtering process. The effect of sputtering after this stage would be limited to the removal of surface layers and oxygen-saturation of new sub-layers at the same time. And thus, keeping the oxygen content practically not changed.

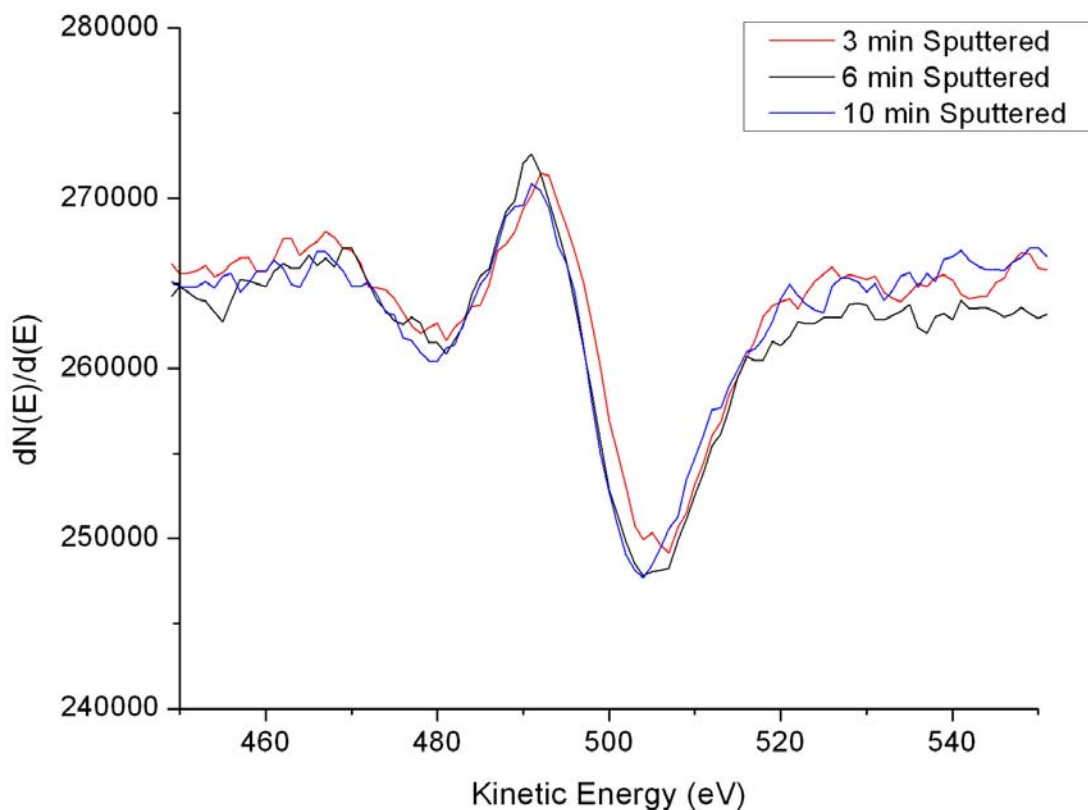


Figure 4.10 AES spectra after different sputtering durations

### Influence of Sputter Time on the Oxygen Signal in AES

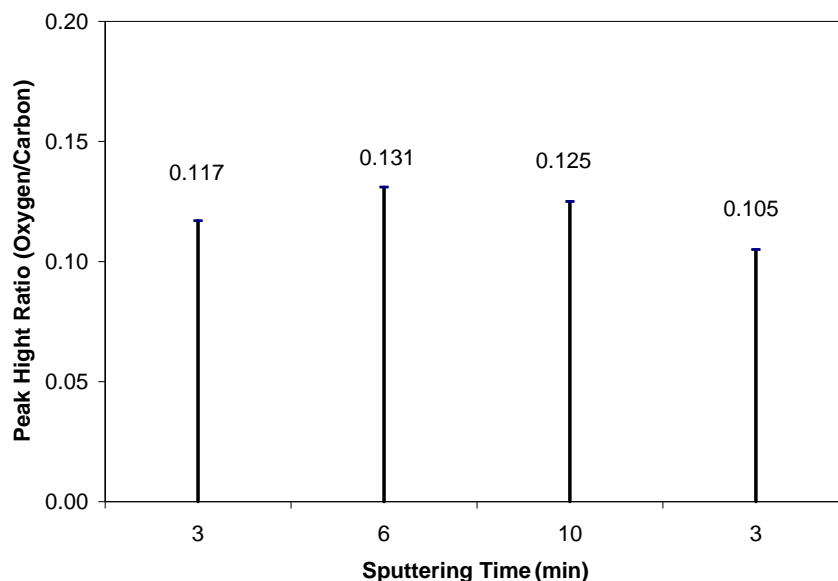


Figure 4.11 AES Peak intensity ratio oxygen/carbon vs. sputtering time

As another measure of the amount of oxygen introduced by the sputtering process, the area under desorption peaks of carbon monoxide and carbon dioxide was investigated for samples which were sputtered for different durations at similar condition.

Figure 4.12 shows the  $C^{18}O$  desorption peaks of carbon monoxide after sputtering the sample for different duration with oxygen/Argon 1:1 mixture. Figure 4.13 shows the desorption peaks of  $C^{18}O_2$  in the same experiments.

As a quantitative measure, in Fig. 4.14, the total representative area (defined as the summation of area under CO desorption peak and 2x area under  $CO_2$  desorption peak) under carbon oxides desorption peaks was calculated and shown for the five successive experiments mentioned in Fig. 4.12 and Fig. 4.13.

In this series, a cleaved annealed HOPG sample was firstly sputtered for 3 minutes after which a TPD experiment was performed. The sample was then sputtered for 6 minutes and TPD experiment was performed and so on.

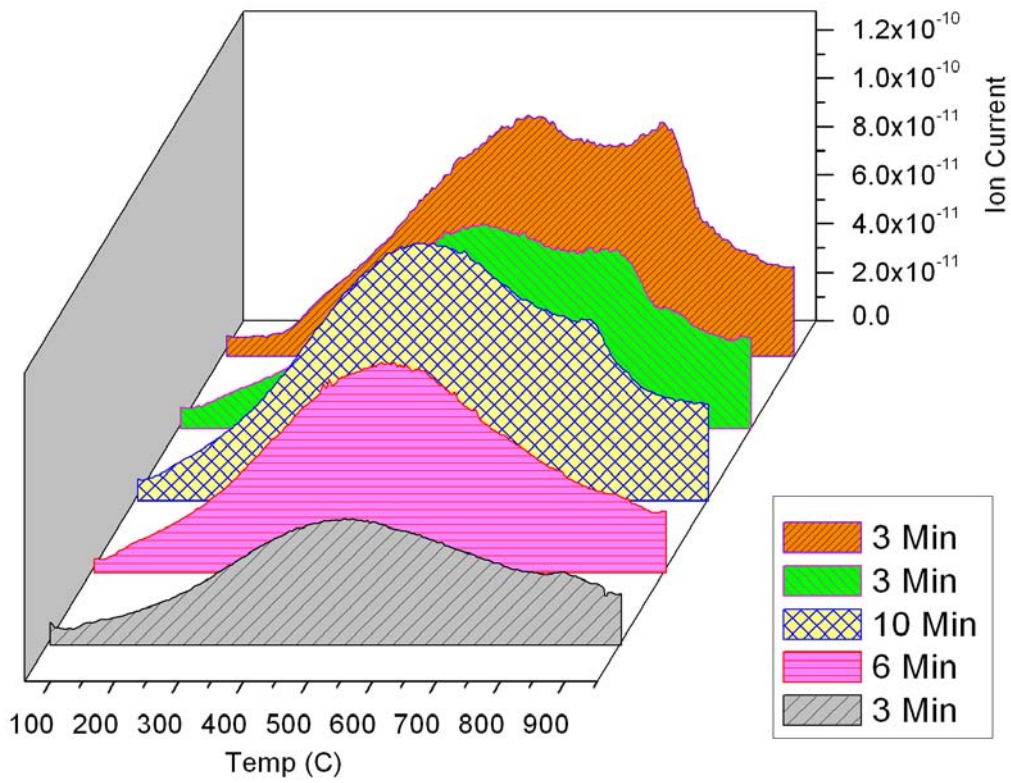


Figure 4.12 CO desorption peaks at different sputtering durations.

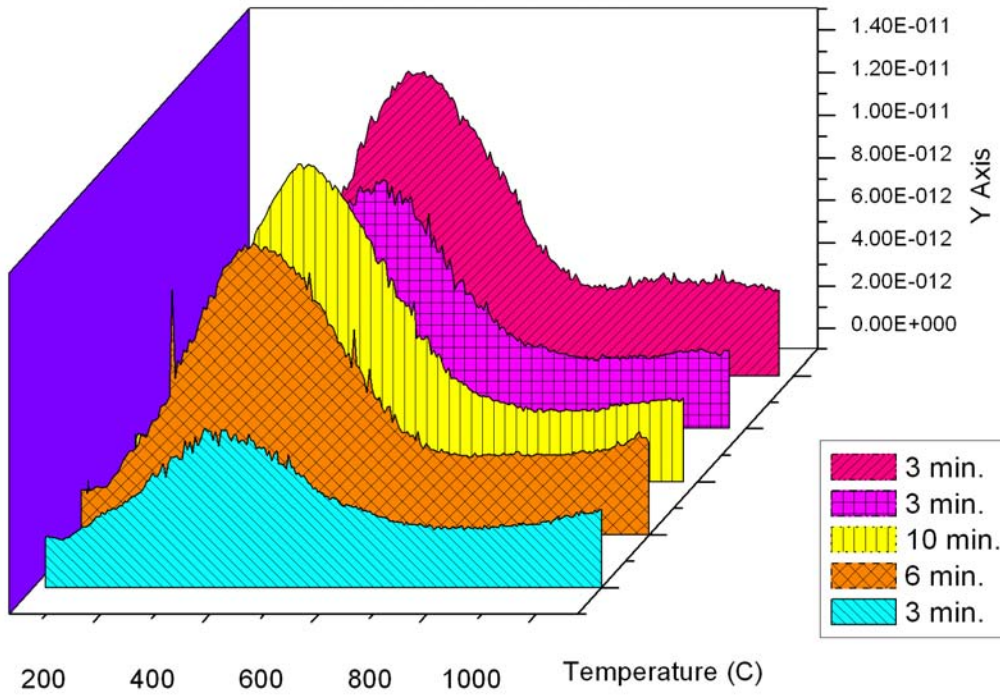


Figure 4.13. CO<sub>2</sub> desorption peaks at different sputtering durations.

In the first three experiments (sputtering times 3, 6 and 10 minutes), as expected, increasing sputtering time has a direct positive influence on the total representative area under carbon oxides desorption peaks. In the 4th experiment, the sample was sputtered again under same conditions for three minutes (same duration of exp.1). Surprisingly, the total representative area under CO<sub>x</sub> desorption peaks, though lower than that obtained after sputtering for 10 minutes, is much higher than that obtained in the first experiment although both experiments involved the same treatment conditions. Repeating this last experiment, additional increase in the total area under CO<sub>x</sub> desorption peaks is obtained.

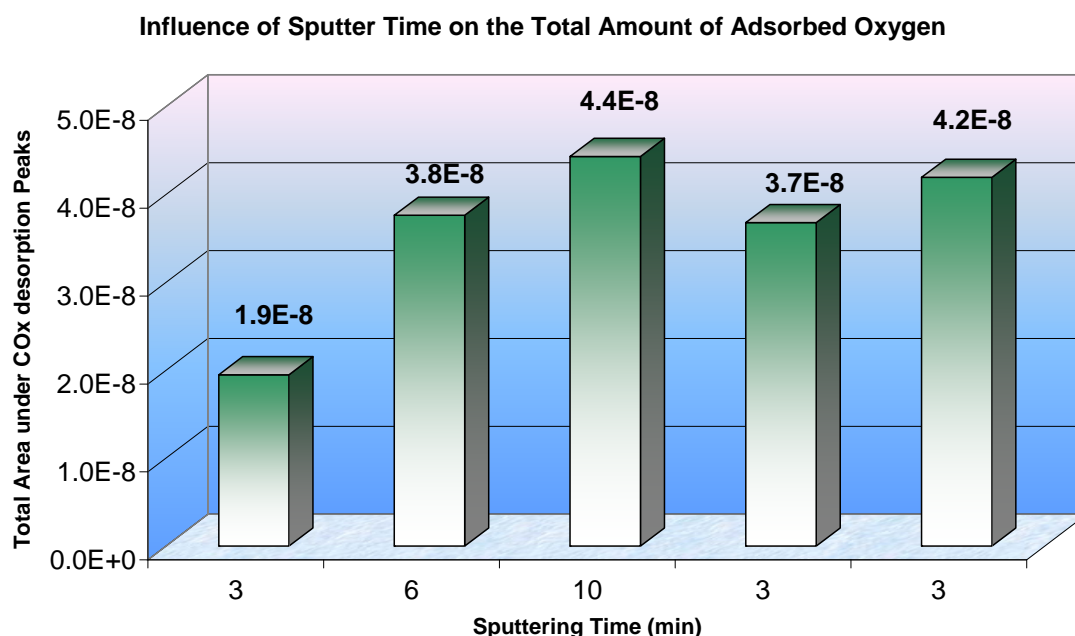


Figure 4.14. Total representative area under CO<sub>x</sub> desorption peaks at different sputtering durations.

From this observation, it is clearly seen that the sputtered surface does not recover after annealing, but in contrast, an irreversible (at the used annealing temperature) destruction of the surface is produced and accumulates after each sputter/anneal treatment. This is shown in figure 4.15 in which the total area under CO<sub>x</sub> desorption peaks of three identical experiments (experiments 1, 4 and 5 in figure 4.14 in which the sample was sputtered for 3 minutes under same conditions) is plotted vs. the accumulated sputtering time.

Now, looking for the influence of accumulated sputtering time on the total representative area under  $\text{CO}_x$  desorption peaks, it is obviously seen that the total amount of oxygen-containing groups is dependent on the accumulative sputtering time. The latter represents the degree of destruction of the surface.

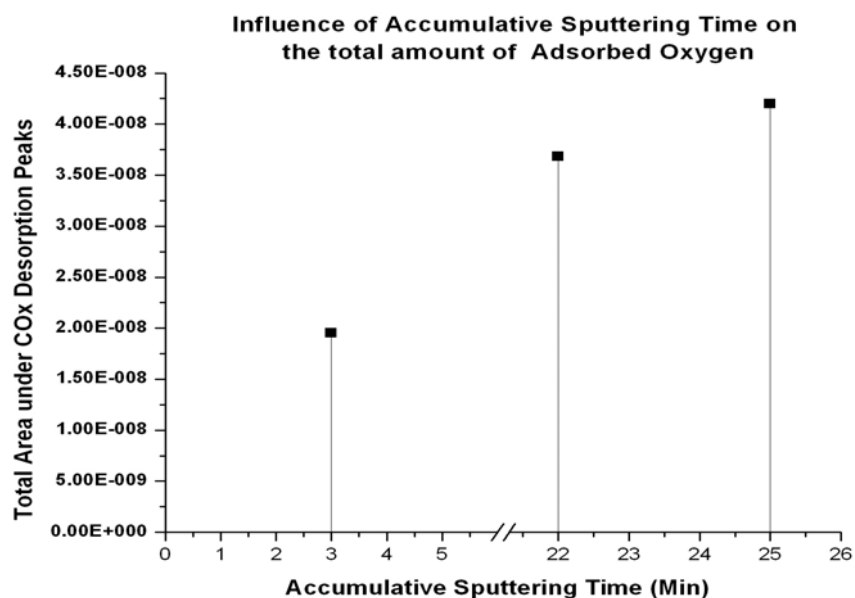


Figure 4.15. Total representative area under  $\text{CO}_x$  desorption peaks vs. accumulative sputtering time

Switching back to figure 4.12, showing several successive sputtering/anneal cycles, it can be seen that a new high-temperature CO desorption peak appeared with a desorption temperature of  $\sim 750^\circ\text{C}$ . It appears in the beginning as a shoulder on the high temperature side of the CO desorption peak. This high-temperature peak grows with repeating experiments and covers the original peak after some time.

The appearance of this peak indicates a significant change in the surface characteristics caused by successive sputter/anneal cycles. This is visible in the SEM image of the surface at this stage (figure 4.16), compared to the cleaved surface, the surface after repeated sputtering is characterized by the presence of large number of pits and pinholes.

The behaviour of the surface upon oxygen exposure experiment at room temperature ( $1 \times 10^{-6}$  mbar  $O_2$ , 90 min) was additionally tested. Although the cleaved surface and the sputtered surface were unable to adsorb oxygen, the surface at this stage was found to be able to –chemically- adsorb molecular oxygen. This chemically adsorbed oxygen, although not detected by Auger spectroscopy (figure 4.17), is clearly seen in TDS experiment as a pure sharp high-temperature  $C^{18}O$  desorption peak at  $750^\circ C$  (figure 4.18). The low-temperature desorption peak of  $C^{18}O$  and the  $C^{18}O_2$  desorption peak were not observed in this case.

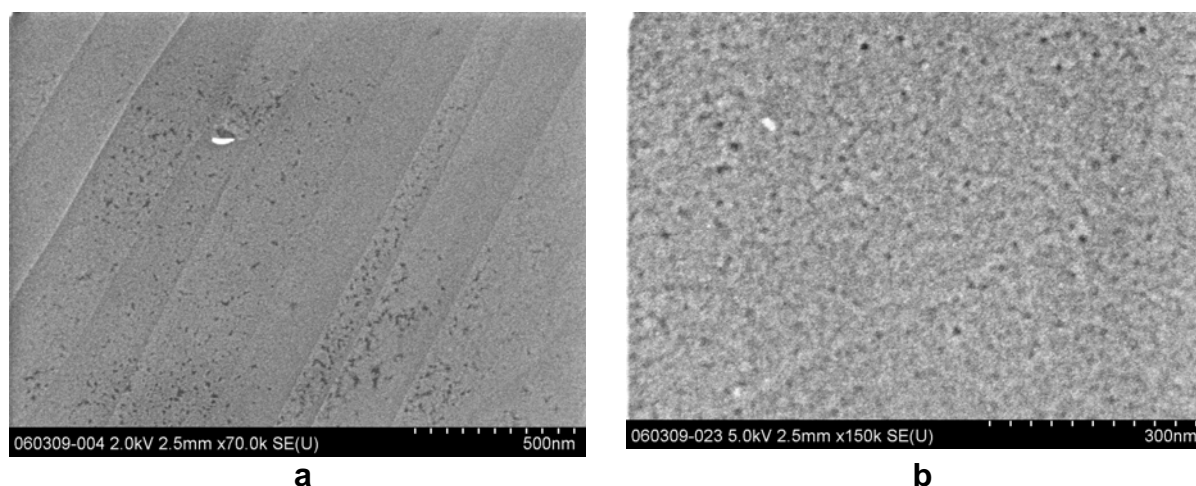


Figure 4.16. SEM images of cleaved HOPG surface (a) and oxygen-sputtered HOPG surface (b)

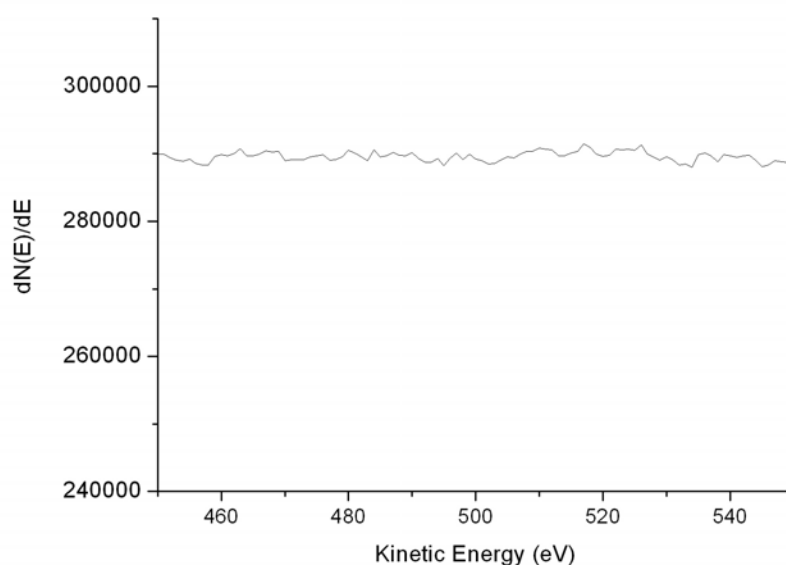


Figure 4.17. Auger after low-temp oxygen adsorption

The exposure of the same (destroyed) surface to molecular oxygen at high temperature (650 °C,  $8 \times 10^{-7}$  mbar  $O_2$ , 120 min) was also investigated. Figure 4.19 shows the TPD spectra obtained after this exposure experiment.

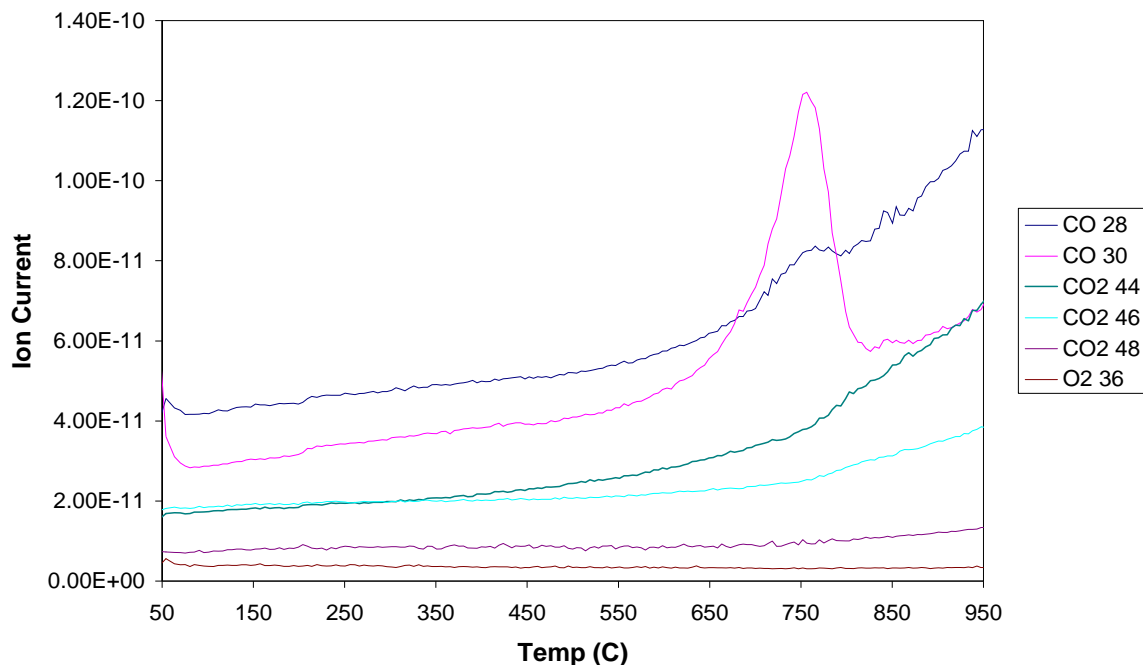


Figure 4.18 TPD spectra after low-temp oxygen adsorption on  $O_2$ -sputtered-annealed HOPG

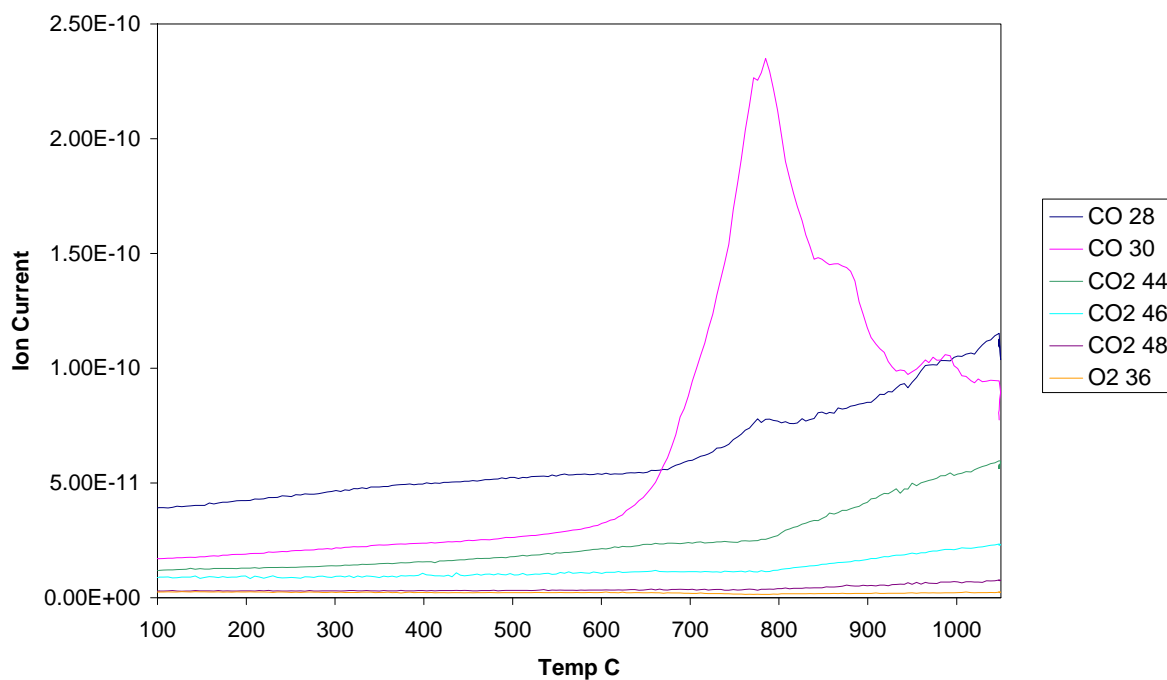


Figure 4.19. TPD after high Temperature oxygen adsorption on  $O_2$ -sputtered-annealed HOPG

In the last treatment, the high-temperature CO desorption peak was detected with a higher intensity than that observed after low temperature exposure experiment.

- (1) Zhuang, Q.; Kyotani, T.; Tomita, A. *Energy Fuels* **1995**, *9*, 630-634.
- (2) Boehm, H. P. *Carbon* **2002**, *40*, 145-149.